CBL-interacting protein kinase 25 contributes to root meristem development

Mukesh Kumar Meena, Niraj Kumar Vishwakarma, Vineeta Tripathi, Debasis Chattopadhyay*

National Institute of Plant Genome Research, Aruna Asaf Ali Marg, New Delhi 110067, India

*Correspondence: Debasis Chattopadhyay, National Institute of Plant Genome Research, Aruna Asaf Ali Marg, New Delhi 110067, India, Ph:+91-11-26735189, Fax:+91-11-26741658, email:debasis@nipgr.ac.in

Highlight: CIPK25, a calcium-regulated protein kinase, plays an important role in the coordination of auxin and cytokinin signaling in root meristem development.

Abstract

Coordination of auxin and cytokinin activities determines root meristem size during post-embryonic development. Calcineurin B-like proteins (CBLs) and their interacting protein kinases (CIPKs) constitute signaling modules that relay calcium signals. Here we report that CIPK25 is involved in regulating the root meristem size. Arabidopsis plants lacking CIPK25 expression displayed a short root phenotype and a slower root growth rate with less meristem cells. This phenotype was rescued by restoration of CIPK25 expression. CIPK25 interacted with CBL4 and -5, and displayed a strong gene expression in the flower and root except in the cell proliferation domain in the root apical meristem. Its expression in root was positively and negatively regulated by auxin and cytokinin, respectively. *cipk25* T-DNA insertion line was compromised in auxin transport and auxin-responsive promoter activity. *cipk25* mutant line showed altered expression of auxin efflux carriers and an Aux/IAA family gene *SHY2*. Decreased PIN1 and PIN2 expression in *cipk25* mutant line was completely restored when combined with SHY2 loss-of-function mutation resulting in recovery of root growth. *SHY2* and *PIN1* expression was partially regulated by cytokinin even in absence of CIPK25, suggesting existence of CIPK25-independent cytokinin signaling pathway(s) as well. Our results suggested a role of CIPK25 in root meristem development.

Key words: auxin, CIPK25, cytokinin, meristem, PIN, root, SHY2

Introduction

Root exhibits indeterminate growth which is regulated by external factors (Schenk and Jackson, 2002; Chapman *et al*., 2012). Root cells are produced in the root apical meristem (RAM) region. Quiescent centre (QC), a group of cells located at the rootward proximal border of RAM is considered as the organizing centre. The cells that surround QC constitute stem cell niche (SCN) that give rise to the different cell files of the root by cell proliferation. Each stem cell divides and the daughter cells undergo additional cycles of division and moves longitudinally towards shoot. Eventually, proliferation rate of these cells decreases as they move upwards; at one point they show a very low probability of division and begin to elongate rapidly at the elongation zone (EZ). For practical convenience, the region between QC and the first elongated cortex cell was considered as RAM in several studies. A small domain of RAM bordering EZ shows a very low probability of cell division, however, yet to start cell elongation is referred to as transition domain (TD). The cells in this domain of RAM grow at the same relative rate as the cells in the proliferative domain and pass to the elongation zone. As cell division rate is different for each cell type, boundary of TD towards QC cannot be well demarcated (Dello Ioio *et al*., 2007; 2008; Ivanov and Dubrovsky, 2013; Perilli and Sabatini, 2010; Verbelen *et al*., 2006). A balance between cell division and differentiation is thus required for proper maintenance of meristem size.

Various phytohormones such as auxin, cytokinin, gibberellin, ethylene and abscisic acid (ABA) play vital roles in maintenance of this balance (reviewed in Pacifici *et al*., 2015). Auxin promotes cell proliferation in RAM through various ways including long- and short-distance signals mediated by polar auxin transporters Pin-Formed (PIN), essential for creating auxin gradients (Tanaka *et al*., 2006). High concentration of auxin promotes SCF^{TIR1}-mediated degradation of Aux/IAA family of transcriptional repressors that form heterodimeric complexes with Auxin Response Factors (ARFs). Aux/IAA degradation releases ARFs from Aux/IAA-mediated repression resulting in activation of auxin-responsive target genes (Boer *et al*., 2014; Kepinski and Leyser, 2005; Mockaitis and Estelle, 2008). On the other hand, cytokinin drastically reduces growth of RAM primarily by promoting cell differentiation (Beemster and Baskin, 2000; Dello Ioio *et al*., 2008). Cytokinin signaling is mediated through a two-component system composed of membrane-localized Arabidopsis Histidine Kinases (AHKs) (Hwang and Sheen, 2001; Inoue *et al*., 2001; To and Kieber, 2008). The signal is

transmitted through phosphorelay to activate Arabidopsis Response Regulators (ARRs) that promote expression of cytokinin-target genes (To *et al*., 2004; To and Kieber, 2008). Transition from mitotic cells in RAM to elongated cells in EZ is accompanied by DNA polyploidization of cells (Dello Ioio *et al*., 2007; Ishida *et al*., 2010; Adachi *et al*., 2011). Cytokinin activates expression of CCS52A1, which promotes DNA polyploidization, through ARR2 and thereby, regulates meristem size (Takahashi *et al*., 2013). It is proposed that the position of the boundary between dividing and elongating zones is determined by the antagonistic interaction of auxin and cytokinin. Cytokinin-activated ARR1 directly activates expression of SHY2/IAA3 resulting in repression of ARF activity and down-regulation of auxin transporter PIN genes causing suppression of cell division. On the other hand, high concentration of auxin promotes degradation of SHY2 and releases ARFs from repression to promote PIN expression and cell division (Dello Ioio *et al*., 2008; Mockaitis and Estelle, 2008). It has been recently shown that in addition to cytokinin-mediated modulation of auxin distribution by regulating PIN expression, cytokinin-dependent auxin degradation also plays important role in positioning transition domain by creating a region of auxin-minima (Di Mambro *et al*., 2017).

Calcium ions (Ca^{2+}) plays a pivotal role in perception of external signals. Increase in free $[Ca^{2+}]_{cyt}$ is recognized by an array of Ca^{2+}-sensors including Calcineurin B-like proteins (CBLs). CBLs in concert with interacting kinases CIPKs (CBL-interacting protein kinases) relay the signal by phosphorylation of various substrates (Luan, 2009). Altered cytosolic Ca^{2+} ($[Ca^{2+}]_{cyt}$)-homeostasis inhibits root cell elongation (Bai *et al*., 2009; Wu *et al*., 2017). Role of Ca^{2+} and calcium-regulated kinases in auxin-signaling has been described in several reports (Monshausen *et al*., 2011; Li *et al*., 2016; Thimann and Schneider, 1939; Takahashi *et al*., 2012; Duby *et al*., 2009; Fuglsang *et al*., 2007; Wang *et al*., 2016; Santin *et al*., 2017). In this study, we observed that Arabidopsis *CIPK25* T-DNA insertion lines exhibited short-root phenotype resulting from reduced RAM size. Restoring expression of *CIPK25* in one of these lines complemented the root phenotype, suggesting this gene plays a role in root development. *CIPK25* expression was responsive to external application of auxin and cytokinin. Mutant lacking *CIPK25* expression displayed compromised auxin transport and low expression of PIN proteins. Short root phenotype of *cipk25* line was restored in SHY2 loss-of function background. Our data suggests CIPK25 plays a role in balancing auxin and cytokinin signaling in root development.

Materials and Methods

Plant materials, growth conditions and treatments

Arabidopsis thaliana wild type (ecotype Columbia; Col-0) and mutant lines (SALK_079011 and SALK_029271) with T-DNA insertions in the exon of *AtCIPK25* (At5g25110) were procured from the Arabidopsis Biological Research Center. Homozygous lines with T-DNA insertions were screened using primers specific for T-DNA borders and *CIPK25* gene. Both SALK_079011 and SALK_029271 lines were used for initial phenotyping study. The remaining experiments were performed with SALK_079011 and designated as *cipk25* mutant. P_{PIN1}*::PIN1-GFP*, *DR5::GUS* and *shy2-24* lines were kindly provided by Dr. Jason W. Reed (University of North Carolina, USA). P_{PIN2}*::PIN2-GFP* and *arr1 arr12* lines were provided by Dr. Ashverya Laxmi (National Institute of Plant Genome Research, India). Above mentioned reporter lines were crossed with *cipk25* mutant. F3/F4 homozygous plants were selected by genotyping and used in the experiments. For stable line generation, *35S::CIPK25*, P_{CIPK25}*::GUS* and P_{SHY2}*::GUS* constructs were introduced in Col-0 plants by agrobacterium mediated floral dip method as described before (Clough and Bent, 1998). P_{CIPK25}*::CIPK25* construct was introduced in *cipk25* mutant plants to generate complementation line. T_3 homozygous P_{SHY2}*::GUS* expressing plants were crossed with *cipk25* mutant for further studies. All seeds were surface-sterilized, stratified and sown on half strength MS media (½MS) plates supplemented with 1% sucrose and 0.8% agar. Arabidopsis plants were grown on agropeat:vermiculite (3:1) mixture in growth chambers with 120 µmol μm^{-2} sec^{-1} light under a 16 h light/8 h dark cycle at 21°C±1°C. For root phenotyping, all plants were grown vertically on ½MS media plates as mentioned above. Root length was marked on plates from 4-day post germination (4 dpg) onwards. Images of 10 dpg-old seedlings were captured for all the plates, root length and per day growth rate was measured for individual seedling using ImageJ software (Abramoff *et al*., 2004).

For analyzing fold expression of *CIPK25* in response to hormones, Col-0 seedlings were transferred to liquid ½MS medium, 12 hrs prior to the treatment for acclamatization. 5µM auxin (IAA) and 5µM t-Zeatin in final concentration were added to liquid medium. Root tissues were collected from treated seedlings at different time interval. For *CIPK25* expression studies in different developmental stages, root tissues were collected from seedlings grown on ½MS plates. CIPK25 promoter activites were analysed in P_{CIPK25}*::GUS* lines at different tissues and developmental stages. Forty-five day old soil-grown plants were taken as matured plants. To determine promoter-reporter activity by staining, seedlings were grown on vertical ½MS plates and treated with hormones for various periods before staining and microscopy.

Expression analysis by Real Time PCR

Plant tissues were ground to a fine powder with liquid N_2, and total RNA was isolated using the TRIzol Reagent (Invitrogen) according to the manufacturers´ protocol. DNA-free total RNA (1 µg) was converted into single-stranded cDNA using oligo-dT_{18} primers and High Fidelity cDNA synthesis kit (Roche Diagnostics GmbH, Germany). Gene-specific primers were designed using the NCBI primer design tool (http://www.ncbi.nlm.nih.gov/tools/primer-blast). For quantitative real time PCR (qRT-PCR), primers were designed to produce 100-150 bp amplicons. qRT-PCR was done in optical 96-well plates on a Vii A 7 Real-Time PCR System (Applied Biosystems, CA, USA) using 2X Power SYBR Green PCR master mix (Applied Biosystems, CA, USA). A dissociation curve analysis was performed for all primer pairs, and all experimental samples yielded a single sharp peak at the amplicon's melting temperature. *ACTIN2* (At3g18780) was used as internal control. Fold induction values of target genes were calculated with the ΔΔCT equation (Rao *et al*., 2013) and presented relative to the mRNA level of target genes in control condition. Technical and biological replicates were used in all the assays. The primer pairs used are listed in Supplementary table S1.

Yeast two-hybrid assay

The CIPK25 full length CDS was fused to the GAL 4 DNA binding domain in pGBKT7-BD vector (Clontech Laboratories Inc). CDS of all CBLs (CBL1-CBL10) of Arabidopsis were cloned into the pGADT7-AD (Clontech Laboratories Inc) to express as fusion with GAL4 activation domain. The pGBKT7-BD and PGADT7-AD constructs were co-introduced into Y2H Gold strain of yeast using Matchmaker Gold yeast Two-Hybrid system kit (Clontech Laboratories Inc). The yeast colonies harboring both the plasmids were selected on double-drop-out (DDO) medium lacking leucine and tryptophan and were confirmed by colony PCR. Positive colonies selected on DDO plate were grown in liquid DDO media for 2 days, adjusted to an OD_{600} of 1, 0.1, 0.01 and 10µl of each dilution were spotted on quadruple drop out (-Leu-Trp-Ade-His) with 2.5mM 3-AT (3-Amino-1,2,4-Triazole). Plates were incubated at 30°C for 5 days.

Transient expression of fusion proteins and microscopic visualization

CIPK25 coding sequence (CDS) was cloned between NcoI and SpeI sites of pCAMBIA1305 vector to generate over-expression lines. To generate *CIPK25* expression line under its native promoter, 2.6 kb promoter and coding region with stop codon was amplified from genomic DNA and cloned in SmaI site of pBI101.2 promoter less vector. For promoter-GUS fusion construct, 2.6 kb fragments upstream to the translation start codon of the corresponding genes were amplified from genomic DNA and were cloned in pBI101.2 vector at BamHI site (for CIPK25 promoter) and SalI/XbaI sites (SHY2 promoter). *35S::CIPK25-YFP* construct

generated by Gateway Technology (Invitrogen) in pEG101 binary vector, was introduced into *Agrobacterium tumefaciens* (GV3101) and infiltrated in *N. benthamiana* leaves for transient expression. For agro infilteration, over-night grown cell cultures were collected and resuspended in 1 ml of infiltration buffer (10mM MES-KOH, pH5.6, 10mM $MgCl_2$, and 150µM acetosyringone) to optical density at 600nm (OD_{600}) to 0.6. The working suspensions were prepared by mixing *Agrobacterium* culture harboring *35S::CIPK25-YFP* construct, organelle markers for plasma membrane (PM-mcherry) (Nelson *et al*., 2007) in (1:1) ratio, incubated at room temperature for 3 hrs and infiltrated into abaxial surface of fully developed leaves. Plants were cultivated for 2 to 3 days under growth room conditions. Subcellular fractionation of CIPK25-YFP expressing plants was done by using Qproteome Cell Compartment kit (Qiagen, GmbH, Germany) by following manufacturer's instructions. Cytosolic, membrane and nuclear protein fractions were separated by SDS-PAGE followed by western blot and probed with anti-GFP (Abcam, UK) antibody. The blotted membrane was probed with the antibodies against the fraction-specific marker proteins e.g. anti-histone H3 (nuclear fraction) (Sigma-Aldrich, Saint Louis, USA), anti-plasma membrane H^+ ATPase (membrane fraction) and anti-cytosolic fructose-1,6-bisphosphatase antibodies (cytosolic fraction) (Agrisera, Sweden).

For GUS reporter staining, Arabidopsis seedlings and different plant tissues were vacuum infiltrated with GUS staining solution (50 mM sodium phosphate buffer (pH 7.0), 2 mM EDTA, 0.12 % Triton, 0.4 mM ferrocyanide, 0.4 mM ferricyanide, 1.0 mM 5-bromo-4-chloro-3-indolyl-beta-D-glucuronide cyclohexylammonium salt) for 5-15 min and incubated in dark at 37°C. The staining time varied between 2 and 12 h depending on the tissue type. Tissues were cleared from chlorophyll by treatment with 70% ethanol at 65°C for 1 h and analyzed by light microscopy.

For bimolecular fluorescence complementation (BiFC) assay, the full-length cDNA fragments (without stop codon) of CBL4, CBL5 and CBL9 were amplified using PCR primers having attB adaptors and cloned into the Gateway entry vector pDONR 207 by BP clonase reaction (Invitrogen). CIPK25 CDS was cloned into pSITE-nEYFP-C1 (CD3-1648) (Martin *et al*., 2009) to generate YFP^N-CIPK25 construct. CBL4, CBL5 and CBL9 were cloned similarly into pSITE-cEYFP-N1 (CD3-1651) to generate CBL4-YFP^C, CBL5-YFP^C and CBL9-YFP^C constructs. *Agrobacterium* strain GV3101 cultures harboring BiFC constructs were infiltrated in *N. benthamiana* leaves as discussed above. For fluorescence quantification, 6 mm leaf discs were cut out of the infiltrated areas and put into a black 96-well plate. Fluorescence intensities of leaf discs were measured in a The FLUOstar® Omega plate reader (BMG LABTECH, Germany) using a 485 ±12 nm excitation and a 520 nm emission filter. To

examine root meristem cells, seedlings were incubated in 10 µg/ml propidium iodide for 5-10 mins, mounted in water, and visualized by Leica TCS SP5 (Leica Microsystems, Wetzlar, Germany) laser-scanning confocal microscope at 535 nm excitation and 617 nm emissions for propidium iodide. Green fluorescence protein (GFP) was visualized at 395 nm excitation and 509 nm emission in P_{PIN1}*::PIN1-GFP* and P_{PIN2}*::PIN2-GFP* expressing roots of Col-0, *cipk25* and *CIPK25OX* seedlings. Agroinfilterated *N. benthamiana* leaf cells for subcellular localization of CIPK25-YFP and plasma membrane marker fused with mCherry were analyzed at 514-527 and 587-610 nm for YFP and mCherry, respectively.

Site-directed mutagenesis, bacterial expression, and kinase assay

Site-directed mutagenesis was done by replacing threonine (T) with aspartic acid (D) at 201th position in CIPK25 as described (Meena *et al*., 2015). The coding regions of CIPK25, CIPK25T/D^{201} were cloned into pGEX-4T2 vector (Amersham Pharmacia Biotech) at SmaI site and transformed into *Escherichia coli* BL21 (DE3)-CodonPlus cells (Stratagene; http://www.stratagene.com/). Recombinant proteins were purified from the bacterial lysates by glutathione–Sepharose affinity chromatography as described before (Gong *et al*., 2002a; b). *In vitro* protein autophosphorylation assays were performed in a 40 µl reaction mixture comprising purified recombinant GST proteins incubated in kinase buffer (10 µCi [γ^{32}P] ATP, 10 µM ATP, 20 mM Tris/HCl pH 8.0, 5 mM $MnCl_2$, 1 mM $CaCl_2$, 0.1 mM EDTA and 1 mM DTT) for 30 min at 30° C. For substrate phosphorylation, MBP (myelin basic protein) was incubated with immunoprecipitated CIPK25 protein from Col-0 seedlings in kinase buffer. The reaction was stopped by addition of 4X SDS-sample buffer. Reaction samples were fractionated by electrophoresis and analysed by autoradiography. CIPK25 protein was detected by specific antibody generated against CIPK25 immunogenic peptide.

Auxin transport assay

Auxin transport was measured essentially as previously described (Shin *et al*., 2005). 5 day-old vertically grown seedlings were used for the experiment. Briefly, agar blocks of 1 mm in diameter containing 7.7×10^{-8} M ^{3}H-IAA (Amersham) were applied at different positions. Agar blocks were placed at root tip for basipetal (shootward) and hypocotyl-root junction for acropetal (rootward) auxin transport. After incubation for 3 hrs, a 0.5 mm section of the root close to the agar block was removed under the microscope. Two consecutive 2-mm segments below the incision line were then collected separately from 15 roots and were pooled and placed into glass scintillation vials containing 5 ml scintillation fluid. The radioactivities in these two pools of root segments were measured using a Perkin Elmer Tri-Carb 2800TR Scintillation counter (Waltham, MA, USA).

Statistical Analysis

Statistical differences between different groups were detected by student's t-test and one-way ANOVA with posthoc SNK test in SigmaStat 2.03. Asterisk or different letters indicate significant difference between genotypes and treatments. Relative root growth rate in presence of external IAA was presented as the percent of growth rate (per day) of the same line in control condition (without IAA).

Results

CIPK25 is involved in root meristem development

We previously reported that overexpression of the chickpea *CIPK25* (*CaCIPK25*) in tobacco (*Nicotiana tabacum*) enhanced root growth (Meena *et al*., 2015). Arabidopsis *CIPK25* (At5g25110.1) is an 1697 bp intron-less gene with coding sequence (CDS) of 1467 bp located between 8657626 and 8659322 bp on chromosome 5. Screening of T-DNA insertion lines (Alonso *et al*., 2003) to investigate the role of Arabidopsis *CIPK25* identified two SALK lines, SALK_079011 (*cipk25-1*) and SALK_029271 (*cipk25-2*) with T-DNA insertion in *CIPK25* coding region having root length shorter by ~40% and ~32%, respectively, as compared to the wild type (Col-0) plants at 8- day post-germination (8 dpg) stage (Fig. 1A). Sequencing of PCR products with T-DNA- and gene-specific primers identified the T-DNA insertions at 902 bp and at 1392 bp downstream to the translation initiation site in *cipk25-1* and *cipk25-2*, respectively. Gene expression analyses by qRT-PCR showed that both the mutant lines did not express significant amount of *CIPK25* mRNA as compared to that in the Col-0 plants (Fig. 1B). The SALK_079011 line was used for further study and designated as *cipk25*. Expression of *CIPK25* full-length CDS under 2.6 kb long native promoter in *cipk25* plants (*cipk25* P_{CIPK25}*::CIPK25*) functionally complemented the short root phenotype as observed in 10-dpg old plants. CIPK25-overexpressing (under CaMV35S promoter) Col-0 lines (*CIPK25OX*, line 1 and 2) displayed ~20% longer roots (Fig. 1C-E), suggesting *CIPK25* is required for root development in Arabidopsis. *CIPK25OX* line 1 was taken for further studies as it showed comparatively better expression and root growth than the other line.

Root lengths and growth rates of the Col-0, *cipk25* and *CIPK25OX* plants were compared over a period of 4 - 9 dpg. No apparent differences were observed in germination rates and germination periods. Measurement of five replicates of fifteen seedlings each showed that the average root length of the mutant line was shorter by 30-36% as compared to the Col-0 plants, whereas that of the *CIPK25OX* line was >11% longer at 9 dpg (Fig. 2A). Root growth

rate, as measured by the increase in the primary root length per day, of the mutant line was ~25% less than the Col-0 plants when measured between 4th and 5th day (Fig. 2B). At the same period the root growth rate of the *CIPK25OX* line was similar to that of the Col-0 plant. Root growth rates of *cipk25* and *CIPK25OX* were ~26% less and ~17% more than the wild type plants, respectively, when measured between 8th and 9th day. To investigate the reason for shorter root length in the mutant line, number of root meristem cells were counted following the method by Perilli and Sabatini, 2010. Propidium iodide-stained roots showed ~18% - 22% less root meristem cell numbers in *cipk25* line as compared to the wild type at 5-9 dpg. At the same period the root meristem cell numbers for *CIPK25OX* line was higher by ~10-20%. However, organization of cells in the root meristematic zone was apparently unperturbed in the mutant line (Fig. 2C, D).

CIPK25 encodes an active protein kinase and interacts with CBL4 and CBL5

To investigate the biochemical character, CIPK25 protein fused with glutathione-S-transferase (GST) was expressed in bacteria. GST-CIPK25 protein showed autophosphorylation activity in *in vitro* reaction. Replacement of a conserved threonine residue with aspartic acid in the activation loop has been shown to increase autophosphorylation activity for various CIPKs (Gong *et al*., 2002a, b). Similarly, substitution of the conserved threonine^{201} residue with aspartic acid resulted in about three-fold enhancement in the autophosphorylation activity of CIPK25. CIPK25 protein immunoprecipitated from Col-0 seedling protein extract showed *in vitro* kinase activity with myelin basic protein (MBP) as substrate, implying plant CIPK25 protein is an active kinase (Fig. 3A). To explore subcellular localization of CIPK25 protein, CIPK25-YFP construct was agroinfiltrated in *N. benthamiana* leaves along with plasma membrane marker PM-mCherry (Nelson *et al*., 2007). Fluorescence overlay showed CIPK25 was localized both in plasma membrane and cytosol (Fig. 3B). To further substantiate localization of CIPK25, subcellular fractionation of transiently expressing CIPK25-YFP in *N. benthamiana* leaves was performed. Presence of CIPK25 was detected by western blot using anti-GFP antibody mostly in membrane and much less in cytosolic fractions, but not in the nuclear fraction (Fig. 3C).

Multiple CBL proteins can interact with a specific CIPK depending on context and this is thought to define distinct signaling pathways (Kolukiasaoglu *et al*., 2004). A yeast-two-hybrid assay was conducted to identify the interacting CBL partners of CIPK25. The full-length CIPK25 protein was found to interact only with CBL4 and CBL5 (Fig. 3D). *In planta* interaction of CIPK25 with CBL4 and CBL5 was investigated by bimolecular fluorescence complementation (BiFC) assay in *N. benthamiana* leaves. Fluorescence due to reconstitution

of yellow fluorescence protein (YFP) was observed when combinations of YFP^N-CIPK25 with CBL4-YFP^C or CBL5-YFP^C were infiltrated in *N. benthamiana* leaves, whereas the combinations of YFP^N-CIPK25 and CBL9-YFP^C did not show any fluorescence (Fig. 3E). Expression of the fused protein in the infiltrated leaf was verified by western blot (Supplementary Fig. S1). To assess the strength of BiFC signals from YFP^N-CIPK25/ CBL4-YFP^C and YFP^N-CIPK25/ CBL5-YFP^C pairs, fluorescence signal intensity of the leaf discs infiltrated with the BiFC constructs were quantified using spectrofluorometer. No significant differences were observed between the BiFC fluorescence signals of YFP^N-CIPK25 with CBL4-YFP^C and CBL5-YFP^C, while the signals fromYFP^N-CIPK25 and CBL9-YFP^C were negligibly low (Fig. 3F).

Tissue-specific expression of *CIPK25*

Expression of *CIPK25* was investigated in different tissues, root growth stages and in response to auxin and cytokinin treatments by qRT-PCR. Expression of *CIPK25* was the lowest in leaves of matured plant and highest in flowers, followed by root and stem (Fig. 4A). Expression of *CIPK25* in root increased gradually from the 4^{th} day to 10^{th} day by ~3 fold, and decreased to ~2.5 fold on 12^{th} day (Fig. 4B). To investigate *in planta* expression pattern, *GUS* reporter gene was cloned under a 2.6 kb 5' upstream regulatory region (including 5' untranslated region) of *CIPK25* (P_{CIPK25}) and expressed in Arabidopsis. GUS activity could be detected throughout the radicles in the germinated seed. GUS activity was observed in cotyledons and hypocotyl except in proliferative region of RAM in a 2 dpg-old seedling. In a 5 day-old seedling, GUS expression initiated at the transition domain and continued to the root-shoot junction. GUS activity in aerial part of a ten day-old seedling was not well pronounced where the blades of young leaves showed low levels of *GUS* expression. GUS activity progressively increased with age in the primary and lateral roots except in the root tip. P_{CIPK25}*::GUS* showed strong expression in the floral organs in adult plants. High level of *CIPK25* expression was detected in carpel, petals and stamens. The ovule was dissected and a strong *CIPK25* promoter activity was observed in ovule integuments, but not in embryo (Fig. 4C). Plant growth hormone auxin (Indole acetic acid/ IAA) positively regulated *CIPK25* expression in root. The transcript level was increased by ~4 fold within 1 h of treatment with 5µM IAA and then slowly decreased to ~1.8-fold within 5h and remained similar till 10 h. In contrast, cytokinin (5 µM trans-Zeatin) treatment downregulated *CIPK25* gene expression by almost ten-fold within 5 h (Fig. 4D). Activation and repression of CIPK25 promoter by auxin and cytokinin treatments was also validated by promoter-reporter assay (Fig. 4E).

cipk25 mutant showed compromised auxin transport and auxin-responsive promoter activity

Cell division and patterning in root are tightly controlled by local concentration of auxin, which is regulated by a process commonly referred to as polar auxin transport. Acropetal (rootward) and basipetal (shootward) modes of auxin transport in root were assayed using radiolabeled indole acetic acid (IAA). The mutant line exhibited reduced acropetal and basipetal auxin transport by ~32% and ~38%, respectively, in comparison to Col-0 plants, while the *CIPK25OX* line displayed similar auxin transport as in the Col-0 by both the modes (Fig. 5A).

External treatment with auxin is known to retard root growth (Eliasson *et al*., 1989). To ascertain the effect of external auxin, 4 day-old seedlings of *cipk25* and Col-0 were transferred to media containing 0.1 µM and 0.5 µM Indole-3-acetic acid (IAA), and incubated for 5 days. Exogenous application of 0.1 µM IAA caused relative root growth rate inhibition in Col-0 seedlings by 65-70%. In contrast, relative root growth rate inhibition of *cipk25* seedlings was 48-60%, suggesting that the mutant was less responsive to auxin-mediated root growth retardation, and a higher concentration of auxin was required for similar effect as in the Col-0. With higher concentration (0.5 µM) of IAA, difference in relative root growth rate retardation between Col-0 and *cipk25* was not significant (Fig. 5B).

Auxin-responsive gene expression in root was assessed by activity of auxin-responsive promoter-reporter *DR_5::GUS*. Col-0 plants with *DR_5::GUS* were crossed with *cipk25* to develop homozygous mutant line expressing *DR_5::GUS* (*cipk25 DR_5::GUS*). GUS activity in the RAM of 5 day-old *cipk25* seedling was much lower than in the Col-0, implying reduced auxin activity in RAM of the mutant line. Further, external application of auxin (5 and 10 µM IAA for 2 hrs) caused weaker induction of auxin-responsive promoter in *cipk25* root as compared to that in Col-0, suggesting a lower auxin transport/signaling in the mutant line (Fig. 5C). A similar contrasting pattern of *DR_5::GUS* activity was observed in case of *agr1-5 pin2* mutant, which was impaired in basipetal auxin transport (Shin *et al*., 2005).

Reduced expression of auxin-responsive genes including auxin-efflux carriers in _cipk25_ root

The PIN auxin efflux carriers control growth and patterning in Arabidopsis root (Blilou *et al*., 2005). Auxin response factors (ARFs) such as, ARF6 and ARF8 were shown as the positive regulators of adventitious root initiation (Guiterrez *et al*., 2012). MONOPTEROS/ARF5 is

required for primary root formation and vascular development (Berleth and Jürgens, 1993; Przemeck *et al*., 1996). ARF7 and ARF19 were shown to regulate lateral root formation (Okushima *et al*., 2007). Expression levels of PINs and ARFs were analyzed by qRT-PCR in roots of Col-0, *cipk25* and *CIPK25OX* plants (Fig. 6A). *PIN1*, *PIN2* and *PIN3* expression levels were down regulated by ~3-fold in *cipk25* seedlings, while ~2-fold reduction was observed for *PIN7*. Out of five ARFs, expression levels of *ARF5*, *ARF6* and *ARF8* were down regulated by >2 fold in the *cipk25* as compared to the wild type plants, whereas, expression levels of *ARF7* and *ARF19*, involved in lateral root formation did not show significant change in *cipk25*. *ARFs* and *PINs*, which showed reduced expression in *cipk25* line exhibited ~1.5-2 fold higher expression levels in the roots of *CIPK25OX* line. Auxin is known to be transported through the central root tissue towards the tip and then redistributed to the cortical tissue and transported basipetally through the epidermis (Petrásek and Friml, 2009; Swarup and Bennett, 2003). The auxin efflux carriers, PIN proteins facilitate this polar auxin transport. PIN1 is thought to promote auxin movement towards the root tip (acropetal) (Blilou *et al*., 2005), whereas basipetal auxin transport is dependent on PIN2 (Müllar *et al*., 1998; Abas *et al*., 2006). To examine the expression of PIN proteins in absence of CIPK25 expression, *cipk25* mutant lines were crossed with reporter lines expressing PIN1 and PIN2 proteins fused with green fluorescence protein (GFP) under their native promoters (P_{PIN1}::*PIN1-GFP* and P_{PIN2}::*PIN2-GFP*). Fluorescence imaging of roots of 5-day old seedlings showed that expression of PIN1 protein was considerably reduced in the stele of the root in *cipk25* background. Similarly, the absence of *CIPK25* caused a significant reduction in PIN2 protein expression in the epidermis. Expressions of GFP-fused PIN1 and -PIN2 were higher in *CIPK25OX* plant (Fig. 6B). All these results suggested that CIPK25 was required for optimal expression of some members of auxin efflux carriers and ARFs.

SHY2 loss-of-function rescued short root phenotype of *cipk25*

The number of cells in root meristem is regulated by auxin and cytokinin, which promote cell division and cell elongation, respectively. SHY2/IAA3 was proposed to act as a point of intersection of auxin- and cytokinin-mediated signaling to regulate root meristem size. Cytokinin represses *PIN1*, *PIN3* and *PIN7* expression to influence root meristem maintenance in a SHY2-dependent manner (Blilou *et al*., 2005; Dello Ioio *et al*., 2008; Tian *et al*., 2002; Vieten *et al*., 2005). As CIPK25 was found to influence root meristem size and PIN expression, *SHY2* expression level was investigated in *cipk25* and was found ~3 fold higher than in the roots of wild type seedlings. This observation was substantiated by *in planta* expression of *SHY2* promoter-GUS fusion construct (P_{SHY2}::*GUS*). *GUS* reporter gene was

cloned under a 2.6 kb long *SHY2* promoter and was expressed in wild type Arabidopsis. It was crossed with *cipk25* line to generate *cipk25* P_{SHY2}*::GUS* line. *SHY2* promoter showed a very weak activity in the transition domain and upwards in wild type background whereas, a high *SHY2* promoter activity was observed in *cipk25* background (Fig. 7A).

We explored influence of SHY2 on *CIPK25* expression by assessing it in SHY2 loss-of-function mutant *shy2-24*. In *shy2-24*, a stop codon was introduced at amino acid position 61, which caused truncation of the protein and mutant was considered as a null mutant for *SHY2* (Tian and Reed, 1999). *CIPK25* expression in *shy2-24* was equivalent to that in Col-0 (Supplementary Fig. S2). To investigate the genetic interaction between CIPK25 and SHY2, a *cipk25 shy2-24* double mutant was generated. The short root phenotype of the *cipk25* plants was completely recovered in the *cipk25 shy2-24* mutant resulting in similar root length as the wild type plants (Fig. 7B). *PIN1*, *PIN2* and *PIN3* expression levels in *cipk25 shy2-24* were found equivalent to the wild type plants (Fig. 7C), indicating that CIPK25 is genetically epistatic to SHY2. Cytokinin treatment downregulated expression of *CIPK25* (Fig. 4D). Cytokinin control of root meristem size is mediated through ARR1 and ARR12 expression in transition domain (Dello Ioio *et al*., 2007, 2008). Absence or over-expression of *CIPK25* did not cause appreciable changes in *ARR1* and *ARR12* expression (Supplementary Fig. S3). Moreover, cytokinin treatment did not change *CIPK25* expression in *arr1 arr12* background, suggesting cytokinin-mediated down-regulation of *CIPK25* expression was dependent on ARR1/ARR12 (Fig. 7D). An analysis of *CIPK25* promoter using PlantPan2.0 (Chow *et al*., 2015) showed a number of potential ARR1- and ARR12-binding sites (Supplementary Table S2). All these observations suggested an involvement of CIPK25 in cytokinin-signaling mediated through ARR1/ARR12.

Cytokinin-mediated down regulation of PIN1 expression in root was shown to be dependent on SHY2 (Dello Ioio *et al*., 2008). To determine whether down-regulation of PIN1 expression by cytokinin is completely dependent on CIPK25, wild type (Col-0) and *cipk25* plants expressing P_{PIN1}::*PIN1-GFP* were treated with 5 µM t-Zeatin. Cytokinin treatment resulted in marked down-regulation of PIN1 protein expression in the wild type background. A reduction in PIN1 expression in *cipk25* roots in control condition was already shown earlier. Treatment with cytokinin further reduced PIN1 expression in the *cipk25* root (Fig. 8A). This observation was substantiated by *PIN1* gene expression in *cipk25* root. Cytokinin treatment resulted in ~3-fold reduction in *PIN1* expression in the wild type root. A similar (~3-fold lower) *PIN1* expression level was observed in control *cipk25*. Cytokinin treatment caused further reduction in *PIN1* expression level in *cipk25* by 1.8-fold (Fig. 8B). Additional reduction in meristematic cell number in *cipk25* after cytokinin treatment corroborated reduced PIN1 expression (Fig.

8C). This result suggested that cytokinin regulates root meristem size by both CIPK25-dependent and –independent pathways.

Discussion

Post-embryonic root growth is maintained by the root apical meristem. Highly proliferative cells of RAM longitudinally move towards shoot and eventually differentiate. Hence, cell division and differentiation rates must be equal to maintain root meristem size and ultimately overall root development. It has been proposed that a balance of auxin and cytokinin signaling regulates the transition of dividing cells to differentiated cells by activating expression of *SHY2* at the transition domain, which subsequently decrease expression of PIN genes (Dello Ioio *et al*., 2008) by suppressing auxin signaling and define the position of the transition domain by reducing auxin transport and additionally, by auxin degradation (Di Mambro *et al*., 2017). It was reported that *SHY2* expression in root was minimal at 3 dpg in an actively growing meristem and reached highest level at 5 dpg, when the meristem reached its final size (Moubayidin *et al*., 2010). With the same analogy *SHY2* expression must also be restricted to maintain equal rate of cell division and rate of transition to elongation. Our results suggest that CIPK25 negatively regulates *SHY2* expression to maintain root meristem size. *CIPK25* expression initiated at TD and was intense in the differentiated zone, and its expression level reached highest when *SHY2* reached its highest expression level after the establishment of meristem. *SHY2* expression is induced by cytokinin treatment in an ARR1-dependent manner (Moubayidin *et al*., 2010), while cytokinin treatment decreased *CIPK25* expression in ARR1/ARR12-dependent manner. A high *SHY2* expression was observed in absence of CIPK25. All these observations suggested an antagonistic relationship between SHY2 and CIPK25. However, application of cytokinin caused further reduction in PIN1 expression and meristem size in *cipk25* mutant suggesting cytokinin also functions in CIPK25-independent pathways. CIPK25-dependent pathway seems to be totally dependent on SHY2 as SHY2 loss of function mutant complemented short root phenotype of *cipk25* and restored expressions of *PIN1*, *PIN2* and *PIN3*. Therefore, CIPK25 may be considered as one of the candidate molecules that balance activities of auxin and cytokinin during root development.

As reported before (Schmid *et al*., 2005), *CIPK25* displayed the highest expression in flowers (Fig. 4). Interestingly, like *ARF6* and *ARF8*, *CIPK25* was also expressed in stamen and gynoecium and its expression was greatly reduced in *arf6 arf8* flowers (Reeves *et al*., 2012). *ARF6* and *ARF8* showed reduced expression in *cipk25* roots. ARF6 and -8 are required for flower maturity and growth of ovule integument (Nagpal *et al*., 2005; Wu *et al*., 2006).

CIPK25 also displayed a high expression in ovule integuments. We did not observe any abnormal phenotype in the flowers of *cipk25* plant. This might be due to the fact that expression of *ARF6* and *ARF8* was only reduced, but not abolished in *cipk25*.

CBL4 and -5 interacted with CIPK25 in yeast-two-hybrid and *in planta* bimolecular fluorescence complementation assay. It is known from several previous reports that an individual CBL protein can interact with multiple CIPKs and *vice-versa* depending on context (Luan, 2009). It is believed that this flexibility of interaction and their sub-cellular localizations are crucial in sensing and responding to specific signal. CBL4 was previously shown to interact with CIPK24 and CIPK6 in the context of salinity stress to modulate activity of Na^+/H^+ antiporter (Qiu *et al*., 2002) and plasma membrane targeting of potassium channel AKT2 (Held *et al*., 2011). Both CBL4 and -5 possess conserved domains for myristoylation and acylation to localize in cell membranes (Batistič *et al*., 2010; Saito *et al*., 2018). Arabidopsis CIPK25 protein, although possesses MG-motif, however, does not undergo N-myristoylation (Saito *et al*., 2018). It is possible that a major pool of the expressed Arabidopsis CIPK25 protein interacted with the corresponding CBL(s) of *N. benthamiana* and was targeted to plasma membrane. CBL sequences possess evolutionarily conserved motifs (Mohanta *et al*., 2015). Cross-species interaction of CIPKs and CBLs was reported before (Tripathi *et al*., 2009; Wang *et al*., 2012). Plasma membrane localization might be essential for CIPK25 function. CIPK11 interacts with CBL5, and myristoylation and acylation of CBL5 was shown to be required for CBL5-CIPK11 complex to phosphorylate guard cell anion channel SLAC1 (Saito *et al*., 2018).

Auxin and cytokinin together regulate various aspects of plant's growth and development. The balance between their interactions is maintained by negative regulation of one signaling pathway by the other. On the other hand, they regulate each other's biosynthesis (Nordstrom *et al*., 2004; Jones *et al*., 2010). The cytokinin biosynthetic gene adenosine triphosphate/adenosine diphosphate isopentyl transferase 5 (IPT5) is rapidly induced by auxin and further induced in SHY2 loss-of-function background, whereas auxin-dependent induction of P_{IPT5}*::GUS* was totally abolished in *SHY2* gain-of-function background (Dello Ioio *et al*., 2008). Relative enhancement of cytokinin activity at the root transition domain might reduce *CIPK25* expression leading to increased *SHY2* expression resulting in reduced auxin signaling. We propose CIPK25 functions genetically above SHY2. Cytokinin-mediated suppression of *CIPK25* expression was dependent on ARR1/ARR12. ARR1 is able to directly regulate *SHY2* expression by binding to and activating *SHY2* promoter (Dello Ioio *et al*., 2008). It is noteworthy that cytokinin was able to suppress PIN1 expression even in absence of CIPK25, suggesting a partial role of CIPK25 in balancing auxin-cytokinin signaling in root meristem development. Presently, it is not clear how CIPK25 functions in auxin/cytokinin-

signaling. Auxin and cytokinin are involved in many interconnected developmental processes through various cross-connected signaling pathways. Therefore, role of CIPK25 in other pathways related to root development cannot be ruled out.

It is known that extracellular application of calcium inhibits cell growth in the transition domain (Ishikawa and Evans, 1992; Legué *et al*., 1997; Fasano *et al*., 2002). Ca^{2+} plays a vital role in polarity and rate of auxin transport through PIN proteins by modulating endo- and exocytosis and direction of PIN localization in plasma membrane (reviewed in Vanneste and Friml, 2013). In this study, we proposed that a Ca^{2+}-regulated protein kinase CIPK25 is involved in regulation of root meristem size by regulating auxin transport through modulating PIN protein expression.

Supplementary Data

Table S1. Primers used in this study.

Table S2. A list of auxin- and cytokinin-responsive elements in CIPK25 promoter.

Fig. S1. Detection of YFP^N-CIPK25, CBL4-YFP^C and CBL9-YFP^C fusion proteins in BiFC assay.

Fig. S2. qRT-PCR analysis of the expression levels of *CIPK25* in *shy2-24* line.

Fig. S3. Relative transcript abundance of *ARR1* and *ARR12* in *cipk25* and *CIPK25OX* seedlings.

Acknowledgements

This project was funded by National Institute of Plant Genome Research (NIPGR), an autonomous institute funded by the Department of Biotechnology (DBT), Government of India and by DBT under the Next Generation Challenge Programme on Chickpea Genomics (grant no. BT/PR12919/AGR/02/676/2009 from 2009-14). Authors acknowledge Dr. J. W. Reed and Dr. Punita Nagpal of Department of Biology, University of North Carolina, Chapel Hill, USA (UNC) for their scientific and technical suggestions and the plant lines and Dr. J. Vadassery, NIPGR for critical reading of the manuscript. MKM, NKV and VT acknowledge Council for Scientific and Industrial Research (CSIR), India and DBT, respectively, for fellowships. The authors are thankful to DBT-eLibrary Consortium (DeLCON) for providing

access to e-Resources. Authors also acknowledge central instrument facility at NIPGR for instrumentation support.

References

Alonso JM, Stepanova AN, Leisse TJ, *et al*. 2003. Genome-Wide Insertional Mutagenesis of *Arabidopsis thaliana*. Science **301,** 653-657.

Abas L, Benjamins R, Malenica N, Paciorek T, Wiśniewska J, Moulinier-Anzola JC, Sieberer T, Friml J, Luschnig C. 2006. Intracellular trafficking and proteolysis of the Arabidopsis auxin-efflux facilitator PIN2 are involved in root gravitropism. Nature Cell Biology. **8,** 249-256.

Abramoff MD, Magalhaes PJ, Ram SJ. 2004. Image processing with ImageJ. Biophotonics International **11,** 36-42.

Adachi S, Minamisawa K, Okushima Y, *et al*. 2011. Programmed induction of endoreduplication by DNA double-strand breaks in Arabidopsis. Proceedings of the National Academy of Sciences, USA **108,** 10004-10009.

Bai L, Zhang G, Zhou Y, Zhang Z, Wang W, Du Y, Wu Z, Song CP. 2009. Plasma membrane-associated proline-rich extensin-like receptor kinase 4 a novel regulator of Ca signalling is required for abscisic acid responses in *Arabidopsis thaliana*. The Plant Journal **60,** 314-327.

Batistič O, Waadt R, Steinhorst L, Held K, Kudla J. 2010. CBL-mediated targeting of CIPKs facilitates the decoding of calcium signals emanating from distinct cellular stores. The Plant Journal **61,** 211-222.

Beemster GT, Baskin TI. 2000. Stunted plant 1 mediates effects of cytokinin but not of auxin on cell division and expansion in the root of Arabidopsis. Plant Physiology **124,** 171-127.

Berleth T, Jürgens G. 1993. The role of the *monopteros* gene in organising the basal body region of the Arabidopsis embryo. Development **118**, 575–587.

Blilou I, Xu J, Wildwater M, Willemsen V, Paponov I, Friml J, Heidstra R, Aida M, Palme K, Scheres B. 2005. The PIN auxin efflux facilitator network controls growth and patterning in Arabidopsis roots. Nature **433,** 39-44.

Boer DR, Freire-Rios A, van den Berg WA, *et al*. 2014. Structural basis for DNA binding specificity by the auxin-dependent ARF transcription factors. Cell **156,** 577-589.

Chapman N, Miller AJ, Lindsey K, Whalley WR. 2012. Roots water and nutrient acquisition: let's get physical. Trends in Plant Science **17,** 701-710.

Chow CN, Zheng HQ, Wu NY, Chien CH, Huang HD, Lee TY, Chiang-Hsieh YF, Hou PF, Yang TY, Chang WC. 2015. PlantPAN 20: an update of plant promoter analysis navigator for reconstructing transcriptional regulatory networks in plants. Nucleic Acids Research **44,** 1154-1160.

Clough SJ, Bent AF. 1998. Floral dip: a simplified method for Agrobacterium-mediated transformation of *Arabidopsis thaliana*. The Plant Journal **16,** 735-743.

Dello Ioio R, Linhares FS, Scacchi E, Casamitjana-Martinez E, Heidstra R, Costantino P, Sabatini S. 2007. Cytokinins determine Arabidopsis root-meristem size by controlling cell differentiation. Current Biology **17,** 678-682.

Dello Ioio R, Nakamura K, Moubayidin L, Perilli S, Taniguchi M, Morita MT, Aoyama T, Costantino P, Sabatini S. 2008. A genetic framework for the control of cell division and differentiation in the root meristem. Science **322,** 1380-1384.

Di Mambro R, De Ruvo M, Pacifici E, *et al*. 2017. Auxin minimum triggers the developmental switch from cell division to cell differentiation in the Arabidopsis root. Proceedings of the National Academy of Sciences, USA **114,** 7641-7649.

Duby G, Poreba W, Piotrowiak D, Bobik K, Derua R, Waelkens E, Boutry M. 2009. Activation of plant plasma membrane H^+-ATPase by 14-3-3 proteins is negatively controlled by two phosphorylation sites within the H^+-ATPase C-terminal region. Journal of Biological Chemistry **284,** 4213-4221.

Eliasson L, Bertell G, Bolander E. 1989. Inhibitory action of auxin on root elongation not mediated by ethylene. Plant Physiology **91,** 310-314.

Fasano JM, Massa GD, Gilroy S. 2002. Ionic signaling in plant responses to gravity and touch. Journal of Plant Growth Regulation **21,** 71-88.

Fuglsang AT, Guo Y, Cuin TA, *et al*. 2007. Arabidopsis protein kinase PKS5 inhibits the plasma membrane H^+-ATPase by preventing interaction with 14-3-3 protein. The Plant Cell **19,** 1617-1634.

Gong D, Gong Z, Guo Y, Chen X, Zhu JK. 2002a. Biochemical and functional characterization of PKS11 a novel Arabidopsis protein kinase. Journal of Biological Chemistry **277,** 28340-28350.

Gong D, Zhang C, Chen X, Gong Z, Zhu JK. 2002b. Constitutive activation and transgenic evaluation of the function of an Arabidopsis PKS protein kinase. Journal of Biological Chemistry **277,** 42088-42096.

Gutierrez L, Mongelard G, Floková K, *et al*. 2012. Auxin controls Arabidopsis adventitious root initiation by regulating jasmonic acid homeostasis. The Plant Cell **24,** 2515-2527.

Held K, Pascaud F, Eckert C, *et al.* 2011. Calcium-dependent modulation and plasma membrane targeting of the AKT2 potassium channel by the CBL4/CIPK6 calcium sensor/protein kinase complex. Cell Research **21,** 1116-1130.

Hwang I, Sheen J. 2001. Two-component circuitry in Arabidopsis cytokinin signal transduction. Nature **413,** 383-389.

Inoue T, Higuchi M, Hashimoto Y, Seki M, Kobayashi M, Kato T, Tabata S, Shinozaki K, Kakimoto T. 2001. Identification of CRE1 as a cytokinin receptor from Arabidopsis. Nature **409,** 1060-1063.

Ishida T, Adachi S, Yoshimura M, Shimizu K, Umeda M, Sugimoto K. 2010. Auxin modulates the transition from the mitotic cycle to the endocycle in Arabidopsis. Development **137,** 63-71.

Ishikawa H, Evans ML. 1992. Induction of curvature in maize roots by calcium or by thigmostimulation: role of the postmitotic isodiametric growth zone. Plant Physiology **100,** 762-768.

Ivanov VB, Dubrovsky JG. 2013. Longitudinal zonation pattern in plant roots: conflicts and solutions. Trends in Plant Science **18,** 237-243.

Jones B, Gunnerås SA, Petersson SV, Tarkowski P, Graham N, May S, Dolezal K, Sandberg G, Ljung K. 2010. Cytokinin regulation of auxin synthesis in Arabidopsis

involves a homeostatic feedback loop regulated via auxin and cytokinin signal transduction. The Plant Cell **22,** 2956-2569.

Kepinski S, Leyser O. 2005. The Arabidopsis F-box protein TIR1 is an auxin receptor. Nature **435,** 446-451.

Kolukiasaoglu U, Weinl S, Blazevic D, Batistic O, Kudla J. 2004. Calcium sensors and their interacting protein kinases: genomics of the Arabidopsis and rice CBL-CIPK signaling networks. Plant Physiology **134,** 43-58.

Legué V, Blancaflor E, Wymer C, Perbal G, Fantin D, Gilroy S. 1997. Cytoplasmic free Ca^{2+} in Arabidopsis roots changes in response to touch but not gravity. Plant Physiology **14,** 789-800.

Li P, Zhao C, Zhang Y, Wang X, Wang X, Wang J, Wang F, Bi Y. 2016. Calcium alleviates cadmium-induced inhibition on root growth by maintaining auxin homeostasis in Arabidopsis seedlings. Protoplasma **253,** 185-200.

Luan S. 2009. The CBL-CIPK network in plant calcium signaling. Trends in Plant Science **14,** 37-42.

Mohanta TK, Mohanta N, Mohanta YK, Parida P, Bae H. 2015. Genome-wide identification of Calcineurin B-Like (CBL) gene family of plants reveals novel conserved motifs and evolutionary aspects in calcium signaling events. BMC Plant Biology **15,** 189.

Martin K, Kopperud K, Chakrabarty R, Banerjee R, Brooks R, Goodin MM. 2009. Transient expression in *Nicotiana benthamiana* fluorescent marker lines provides enhanced definition of protein localization movement and interactions *in planta*. The Plant Journal **59,** 150-162.

Meena MK, Ghawana S, Dwivedi V, Roy A, Chattopadhyay D. 2015. Expression of chickpea CIPK25 enhances root growth and tolerance to dehydration and salt stress in transgenic tobacco. Frontiers in Plant Science **6,** 683.

Mockaitis K, Estelle M. 2008. Auxin receptors and plant development: a new signaling paradigm. Annual Review of Cell and Developmental Biology **24,** 55-80.

Monshausen GB, Miller ND, Murphy AS, Gilroy S. 2011. Dynamics of auxin-dependent Ca^{2+} and pH signaling in root growth revealed by integrating high-resolution imaging with automated computer vision-based analysis. The Plant Journal **65,** 309-318.

Moubayidin L, Perilli S, Dello Ioio R, Di Mambro R, Costantino P, Sabatini S. 2010. The rate of cell differentiation controls the Arabidopsis root meristem growth phase. Current Biology **20,** 1138-1143.

Müller A, Guan C, Gälweiler L, Tänzler P, Huijser P, Marchant A, Parry G, Bennett M, Wisman E, Palme K. 1998. AtPIN2 defines a locus of Arabidopsis for root gravitropism control. The EMBO Journal **17,** 6903-6911.

Nagpal P, Ellis CM, Weber H, *et al*. 2005. Auxin response factors ARF6 and ARF8 promote jasmonic acid production and flower maturation. Development **132,** 4107-4118.

Nelson BK, Cai X, Nebenfùhr A. 2007. A multicolored set of *in vivo* organelle markers for colocalization studies in Arabidopsis and other plants. The Plant Journal **51,** 1126-1136.

Nordström A, Tarkowski P, Tarkowska D, Norbaek R, Astot C, Dolezal K, Sandberg G. 2004. Auxin regulation of cytokinin biosynthesis in *Arabidopsis thaliana*: a factor of potential

importance for auxin-cytokinin-regulated development. Proceedings of the National Academy of Sciences, USA **101,** 8039-8044.

Okushima Y, Fukaki H, Onoda M, Theologis A, Tasaka M. 2007. ARF7 and ARF19 regulate lateral root formation via direct activation of LBD/ASL genes in Arabidopsis. The Plant Cell **19,** 118-130.

Pacifici E, Polverari L, Sabatini S. 2015. Plant hormone cross-talk: the pivot of root growth. Journal of Experimental Botany **66,** 1113-1121.

Perilli S, Sabatini S. 2010. Analysis of root meristem size development. Methods in Molecular Biology **655,** 177-187.

Petrásek J, Friml J. 2009. Auxin transport routes in plant development. Development **136,** 2675-2688.

Przemeck GK, Mattsson J, Hardtke CS, Sung ZR, Berleth T. 1996. Studies on the role of the Arabidopsis gene *MONOPTEROS* in vascular development and plant cell axialization. Planta **200**, 229–237.

Qiu QS, Guo Y, Dietrich MA, Schumaker KS, Zhu JK. 2002. Regulation of SOS1, a plasma membrane Na^+/H^+ exchanger in *Arabidopsis thaliana*, by SOS2 and SOS3. Proceedings of the National Academy of Sciences, USA **99,** 8436-8441.

Rao X, Huang X, Zhou Z, Lin X. 2013. An improvement of the 2ˆ-delta delta CT method for quantitative real-time polymerase chain reaction data analysis. Biostatistics, Bioinformatics and Biomathematics **3,** 71-85.

Reeves PH, Ellis CM, Ploense SE, *et al.* 2012. A regulatory network for coordinated flower maturation. PLoS Genetics **8,** e1002506.

Saito S, Hamamoto S, Moriya K, *et al.* 2018. N-myristoylation and S-acylation are common modifications of Ca^{2+} -regulated Arabidopsis kinases and are required for activation of the SLAC1 anion channel. New Phytologist **218,** 1504-1521.

Santin F, Bhogale S, Fantino E, Grandellis C, Banerjee AK, Ulloa RM. 2017. *Solanum tuberosum* StCDPK1 is regulated by miR390 at the posttranscriptional level and phosphorylates the auxin efflux carrier StPIN4 in vitro a potential downstream target in potato development. Physiologia Plantarum **159,** 244-261.

Schenk HJ, Jackson RB. 2002. Rooting depths lateral root spreads and below-ground/above-ground allometries of plants in water-limited ecosystems. Journal of Ecology **90,** 480-494.

Schmid M, Davison TS, Henz SR, Pape UJ, Demar M, Vingron M, Schölkopf B, Weigel D, Lohmann JU. 2005. A gene expression map of *Arabidopsis thaliana* development. Nature Genetics **37,** 501-506.

Shin H, Shin HS, Guo Z, Biancaflor EB, Masson PH, Chen R. 2005. Complex regulation of Arabidopsis AGR1/PIN2-mediated root gravitropic response and basipetal auxin transport by catharidin-sensitive protein phosphatases. The Plant Journal **42,** 188-200.

Swarup R, Bennett M. 2003. Auxin transport: the fountain of life in plants? Developmental Cell **5,** 824-826.

Takahashi K, Hayashi K, Kinoshita T. 2012. Auxin activates the plasma membrane H^+-ATPase by phosphorylation during hypocotyl elongation in Arabidopsis. Plant Physiology **159,** 632-641.

Takahashi N, Kajihara T, Okamura C, Kim Y, Katagiri Y, Okushima Y, Matsunaga S, Hwang I, Umeda M. 2013. Cytokinins control endocycle onset by promoting the expression of an APC/C activator in Arabidopsis roots. Current Biology **23,** 1812-1817.

Tanaka H, Dhonukshe P, Brewer PB, Friml J. 2006. Spatiotemporal asymmetric auxin distribution: a means to coordinate plant development. Cellular and Molecular Life Sciences **63,** 2738-2754.

Thimann KV, Schneider CA. 1939. The relative activities of different auxins. American Journal of Botany **26,** 328-333.

Tian Q, Reed JW. 1999. Control of auxin-regulated root development by the *Arabidopsis thaliana* SHY2/IAA3 gene. Development **126,** 711-721.

Tian Q, Uhlir NJ, Reed JW. 2002. Arabidopsis SHY2/IAA3 inhibits auxin-regulated gene expression. The Plant Cell **14,** 301-319.

To JP, Haberer G, Ferreira FJ, Deruère J, Mason MG, Schaller GE, Alonso JM, Ecker JR, Kieber JJ. 2004. Type-A Arabidopsis response regulators are partially redundant negative regulators of cytokinin signaling in Arabidopsis. The Plant Cell **16,** 658-671.

To JP, Kieber JJ. 2008. Cytokinin signaling: two-components and more. Trends in Plant Science **13,** 85-92.

Tripathi V, Parasuraman B, Laxmi A, Chattopadhyay D. 2009. CIPK6, a CBL-interacting protein kinase is required for development and salt tolerance in plants. The Plant Journal **58,** 778-790.

Vanneste S, Friml J. 2013. Calcium: The Missing Link in Auxin Action. Plants Basel **2,** 650-675.

Verbelen JP, De Cnodder T, Le J, Vissenberg K, Baluska F. 2006. The Root Apex of *Arabidopsis thaliana* consists of four distinct zones of growth activities: Meristematic Zone, Transition Zone, Fast Elongation Zone, and Growth Terminating Zone. Plant Signaling & Behavior **1,** 296-304.

Vieten A, Vanneste S, Wisniewska J, Benkova E, Benjamins R, Beekman T, Luschnig C, Friml J. 2005. Functional redundancy of PIN proteins is accompanied by auxin-dependent cross-regulation of PIN expression. Development **132,** 4521-4531.

Wang F, Chen ZH, Liu X, Colmer TD, Zhou M, Shabala S. 2016. Tissue-specific root ion profiling reveals essential roles of the CAX and ACA calcium transport systems in response to hypoxia in Arabidopsis. Journal of Experimental Botany **67,** 3747-3762.

Wang RK, Li LL, Cao ZH, Zhao Q, Li M, Zhang LY, Hao YJ. 2012. Molecular cloning and functional characterization of a novel apple MdCIPK6L gene reveals its involvement in multiple abiotic stress tolerance in transgenic plants. Plant Molecular Biology **79,** 123-135.

Wu MF, Tian Q, Reed JW. 2006. Arabidopsis microRNA167 controls patterns of ARF6 and ARF8 expression and regulates both female and male reproduction. Development **133,** 4211-4218.

Wu J, Wang Y, Kim SG, Jung KH, Gupta R, Kim J, Park Y, Kang KY, Kim ST. 2017. A secreted chitinase-like protein OsCLP supports root growth through calcium signaling in *Oryza sativa*. Physiologia Plantarum **161,** 273-284.

Figure legends

Fig. 1. *cipk25* mutant exhibits shorter root length phenotype. (A) Primary root length phenotype of 8 dpg old Col-0, *cipk25-1* and *cipk25-2* mutants vertically grown on ½MS medium. Lower panel shows root length measurement of three replicate experiments with fifteen seedlings for each replicate of each genotype. Error bars are SD±. Statistically significant differences between root length of Col-0 and *cipk25* mutants were analysed by unpaired t-test: *P ≤ 0.05, **P ≤ 0.001. (B) Schematic representation of CIPK25 gene structure and T-DNA insertion sites of *cipk25-1* and *cipk25-2* mutants. Lower panel shows relative transcript level of *CIPK25* in 8 dpg old Col-0 and *cipk25* mutants by qRT- PCR. *ACTIN2* was used as control. Error bars indicate SD± of three replicates. Significant differences was calculated by unpaired t-test: **P ≤ 0.001. (C) Root length phenotype of 10 dpg old Col-0, *cipk25*, *cipk25* P_{CIPK25}*::CIPK25*, *CIPK25OX-1* and *CIPK25OX-2* lines. (D) *CIPK25* relative transcript levels in 10 dpg old Col-0, *cipk25*, *cipk25* P_{CIPK25}*::CIPK25*, *CIPK25OX-1* and *CIPK25OX-2* seedlings. *ACTIN2* was used as endogenous control. Different letters indicate significant differences (ANOVA; P ≤ 0.05). (E) Root length comparison of 10 dpg old Col-0, *cipk25*, *cipk25* P_{CIPK25}*::CIPK25*, *CIPK25OX-1* and *CIPK25OX-2* seedlings. Error bars are in SD±, n=30.

Fig. 2. *cipk25* mutant exhibits slower root growth rate and less root meristem cell number. (A) and (B) Primary root length and growth rate (mm/day) measurements of Col-0, *cipk25* and *CIPK25OX* seedlings vertically grown on ½MS medium. Values are SD± of seventy five samples for each genotype. Different letters indicate significant differences (ANOVA; P ≤ 0.05) at 9 dpg and 8-9 dpg old seedlings for root length and growth rate. (C) Meristem cell number count in Col-0, *cipk25* and *CIPK25OX* in 5, 7 and 9 dpg old seedlings. Error bars are SD± of n=20. Different letters indicate statistically significant differences among 9 dpg old seedlings (ANOVA; P ≤ 0.05). (D) Propidium iodide-stained primary roots of 5 dpg old Col-0, *cipk25* and *CIPK25OX* seedlings. White and yellow arrows indicate quiescent center (QC) and the first elongated cortex cell, respectively.

Fig. 3. CIPK25, an active protein kinase, interacts with CBL4 and 5 *in planta*. (A) Autophosphorylation assay of bacterially expressed GST- CIPK25 and CIPK25T/D^{201} proteins. Below is the Coomassie blue-stained gel. Lower panel is showing substrate phosphorylation of MBP by immunoprecipitated CIPK25 protein from Col-0 and *cipk25* mutant seedlings. Western blot of CIPK25 was shown. (B) Visualization of CIPK25-YFP fusion protein in agroinfiltrated leaves of *N. benthamiana* co-infiltrated with plasma membrane marker PM-mCherry. Magnified view of merged image in lower panel showing CIPK25 localization at plasma membrane (yellow line) and cytoplasm (green line). (C) Western blot showing subcellular fractions of CIPK25-YFP expressing *N. benthamiana* leaves. The blot was probed with antibodies against GFP for CIPK25, plasma membrane (PM) H^+-ATPase, cytosolic fructose-1,6-bisphosphatase (cFBPase) and H3 histone. (D) Yeast-two-hybrid interaction study of CIPK25 and CBLs. Y2H gold yeast cells were co-transformed with pGBKT7-CIPK25 and pGADT7-CBL1-10 and auxotrophic selection was carried out to detect protein-protein interaction. (E) Interactions between CIPK25 and CBL4/CBL5 *in planta* was shown by BiFC assay. CIPK25 fused with N-terminal domain of YFP (YFP^N) and CBL4/CBL5/CBL9 fused with C-terminal domain of YFP (YFP^C) were transiently expressed in *N. benthamiana* by agroinfiltration. Images show YFP-mediated fluorescence derived from the protein-protein interaction. Bar = 100 µm. Infiltration of CBL9-YFP^C with YFP^N-CIPK25 was used as negative control. Expression of the proteins is shown in Fig. S1. (F) Yellow fluorescence intensity within leaf discs expressing YFP^N-CIPK25 with CBL4-YFP^C, CBL5-YFP^C or CBL9-YFP^C. Different letters denote significant differences among samples based on SNK test (n=8, ANOVA; $P \leq 0.05$).

Fig. 4. *CIPK25* gene expression profiles at in different tissues, root growth stages and in response to hormone treatments. CIPK25 gene expression in different tissues (A) and in different root growth stages (B) analyzed by qRT-PCR. *ACTIN2* expression was used for normalization. Error bars SD±, n=3. Different letters indicate significant differences among samples (ANOVA; $P \leq 0.05$). (C) CIPK25 promoter activities were investigated with promoter::reporter gene (GUS) constructs expressed in transgenic plants. Histochemical GUS stainings are shown for (i) radicle of germinating seedling; (ii) 2 dpg old seedling; (iii) primary root tip of 5 dpg old seedling (Arrow indicates first elongated cortex cell); (iv) 10 dpg old seedling; (v) flower; (vi) gynoecium; (vii) immature seeds with embryo; (viii) embryo. (D) Fold change in *CIPK25* expression as analysed by qRT-PCR in roots of 10 dpg old Col-0 seedlings treated with 5µM IAA and 5µM t-Zeatin for different time interval. *ACTIN2* expression was used for normalization. Error bars SD±, n=3. Different letters indicate significant differences among samples (ANOVA; $P \leq 0.05$). (E) *pCIPK25::GUS*

expression was visualized in primary roots of 10 dpg old seedlings treated with 5µM IAA for 1 hr and 5µM t-Zeatin for 5hr.

Fig. 5. Auxin transport and auxin-responsive promoter assays in *cipk25*. (A) Comparison of acropetal (rootward) and basipetal (shootward) root auxin transport in 5 dpg old Col-0, *cipk25* and *CIPK25OX* seedlings in a root segment 2 mm below (in acopetal) or above (in basipetal) the site of ^{3}H-IAA application. Data are presented as the percentage auxin transport relative to Col-0. Error bars are SD±, t-test (*P ≤ 0.05) of three measurements of 15 seedlings each. (B) Auxin-mediated root growth rate retardation of Col-0 and *cipk25* in response to 0.1 µM and 0.5 µM auxin treatments. 4 dpg old Col-0, *cipk25* mutant seedlings grown on ½ MS medium were transferred to IAA-free or IAA-containing medium, and grown for an additional 5 days. Relative root growth rate in presence of external IAA was presented as the percent of growth rate (per day) of the same line in control condition (without IAA). The error bars represents SD±, t-test (*P ≤ 0.05), with three replicates of 10 seedlings each. (C) Auxin responsive promoter activity using *DR$_5$::GUS* in Col-0 and *cipk25* mutant. 5 dpg old seedlings were treated with 5µM and 10µM IAA for 2 hrs and stained for GUS activity.

Fig. 6. Expression of auxin response factors (ARFs) and efflux carriers (PINs) in *cipk25*. (A) Relative transcript levels of auxin response factors (*ARF5*, *ARF6*, *ARF7*, *ARF8* and *ARF19*) and efflux carriers (PIN1, PIN2, PIN3 and PIN7) were analyzed by qRT-PCR in roots of 5 dpg old Col-0, *cipk25* and *CIPK25OX* seedlings. *ACTIN2* expression was used for normalization. Error bars represents SD± of three biological replicates with fifteen seedlings for each genotype. (B) Visualization of expressions of auxin efflux carriers PIN1 and PIN2. Fluorescence images from the GFP fusion proteins expressed through the native promoters of individual genes in Col-0, *cipk25* and *CIPK25OX* background. 5 dpg old seedlings were stained with propidium iodide to explore meristem cell profiles and analysed by confocal microscope. Scale bar in confocal images = 100µm. White and yellow arrows indicate quiescent center (QC) and the first elongated cortex cell, respectively.

Fig. 7. Genetic interaction of *CIPK25* and *SHY2*. (A) Relative transcript abundance of *SHY2* in 5 dpg old Col-0 and *cipk25* mutant roots was analysed by qRT-PCR and semi-quantitative RT-PCR. *ACTIN2* was used as internal control. Right panel shows histochemical GUS staining of primary roots of 5 dpg-old seedlings expressing GUS reporter under *SHY2*

promoter. Arrow shows the first elongated cortex cell. (B) Primary root length phenotype of 10 dpg-old Col-0, *cipk25*, *shy2-24* and *cipk25 shy2-24* mutants vertically grown on ½ MS medium. Right panel shows root length measurement. Error bars represent SD±, n=24. (C) Relative transcript levels of auxin efflux carriers were analysed by qRT-PCR in roots of 5 dpg old Col-0, *cipk25*, *shy2-24* and *cipk25 shy2-24* seedlings. Different letters indicate statistically significant differences by ANOVA, $P \leq 0.05$. Error bars are SD±, n=3. (D) qRT-PCR analysis of the expression levels of *CIPK25* in roots of 10 dpg-old Col-0 and *arr1 arr12* seedlings treated with 5µM t-Zeatin for different time interval. *ACTIN2* expression was used as internal control. Error bars are SD±, n=3.

Fig. 8. Cytokinin-responsive PIN1 expression in *cipk25*. (A) Fluorescence images of auxin efflux carrier PIN1-GFP fusion protein driven through its native promoter in Col-0 and *cipk25* seedlings in control condition and in response to cytokinin treatment (5 µM t-Zeatin, 6 hours). Roots of 5 dpg-old seedlings were stained with propidium iodide (PI) for visualizing root cells. White and yellow arrows indicate quiescent center (QC) and the first elongated cortex cell, respectively. Scale bar =100µM. (B) Relative transcript levels of *PIN1* was analysed by qRT-PCR in roots of 5 dpg-old Col-0 and *cipk25* seedlings in control and treated with cytokinin (5 µM t-Zeatin, 6 hours). Error bars are SD± of 3 biological replicates, ANOVA, $P \leq 0.05$. (C) Meristem cell number count in 5 dpg-old Col-0 and *cipk25* seedlings in control condition and in response to cytokinin treatment (5 µM t-Zeatin, 12 hours). Values are mean ± SD of twenty samples each. Different letters indicate significant differences among samples (ANOVA, $P \leq 0.05$).

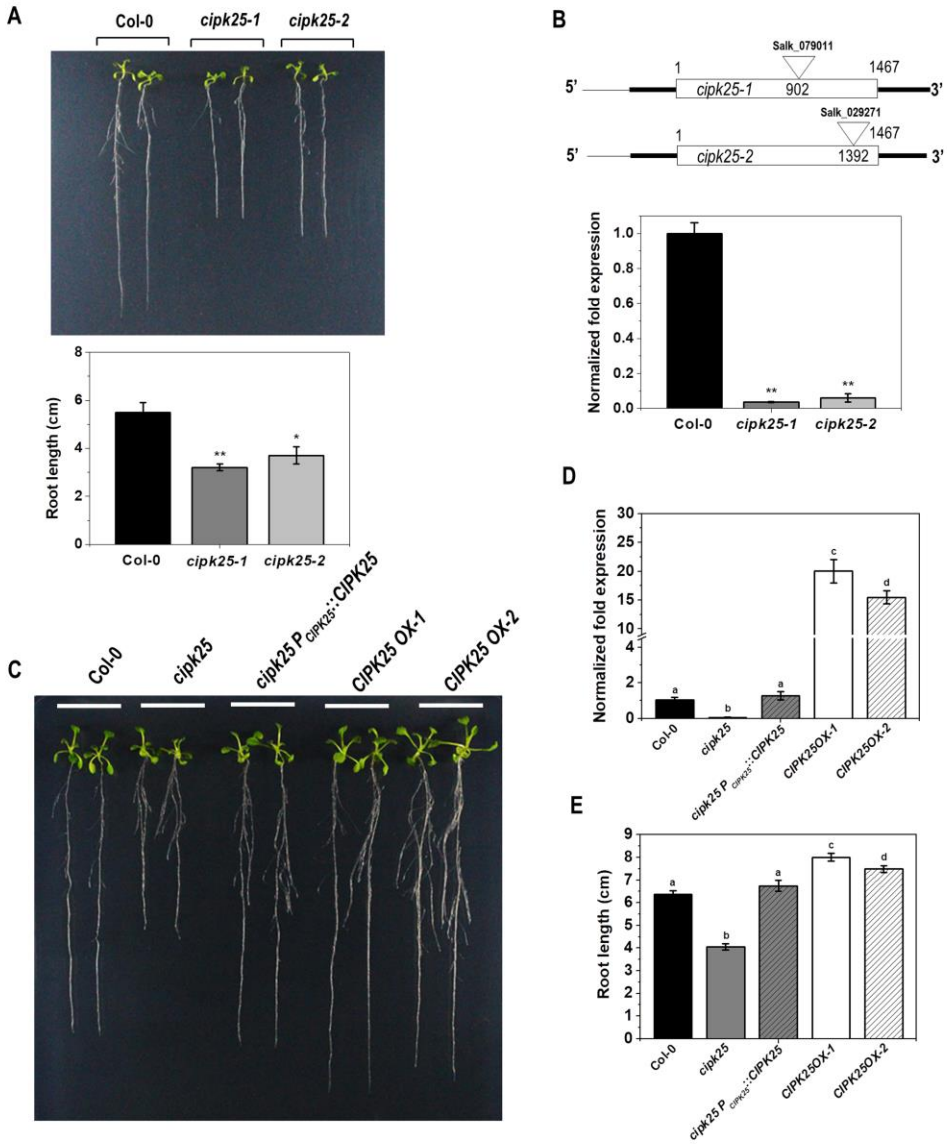

Fig. 1. *cipk25* mutant exhibits shorter root length phenotype. (A) Primary root length phenotype of 8 dpg old Col-0, *cipk25-1* and *cipk25-2* mutants vertically grown on ½MS medium. Lower panel shows root length measurement of three replicate experiments with fifteen seedlings for each replicate of each genotype. Error bars are SD±. Statistically significant differences between root length of Col-0 and *cipk25* mutants were analysed by unpaired t-test: *P ≤ 0.05, **P ≤ 0.001. (B) Schematic representation of CIPK25 gene structure and T-DNA insertion sites of *cipk25-1* and *cipk25-2* mutants. Lower panel shows relative transcript level of *CIPK25* in 8 dpg old Col-0 and *cipk25* mutants by qRT- PCR. *ACTIN2* was used as control. Error bars indicate SD± of three replicates. Significant differences was calculated by unpaired t-test: **P ≤ 0.001. (C) Root length phenotype of 10 dpg old Col-0, *cipk25*, *cipk25* P_{CIPK25}*::CIPK25*, *CIPK25OX-1* and *CIPK25OX-2* lines. (D) *CIPK25* relative transcript levels in 10 dpg old Col-0, *cipk25*, *cipk25* P_{CIPK25}*::CIPK25*, *CIPK25OX-1* and *CIPK25OX-2* seedlings. *ACTIN2* was used as endogenous control. Different letters indicate significant differences (ANOVA; P ≤ 0.05). (E) Root length comparison of 10 dpg old Col-0, *cipk25*, *cipk25* P_{CIPK25}*::CIPK25*, *CIPK25OX-1* and *CIPK25OX-2* seedlings. Error bars are in SD±, n=30.

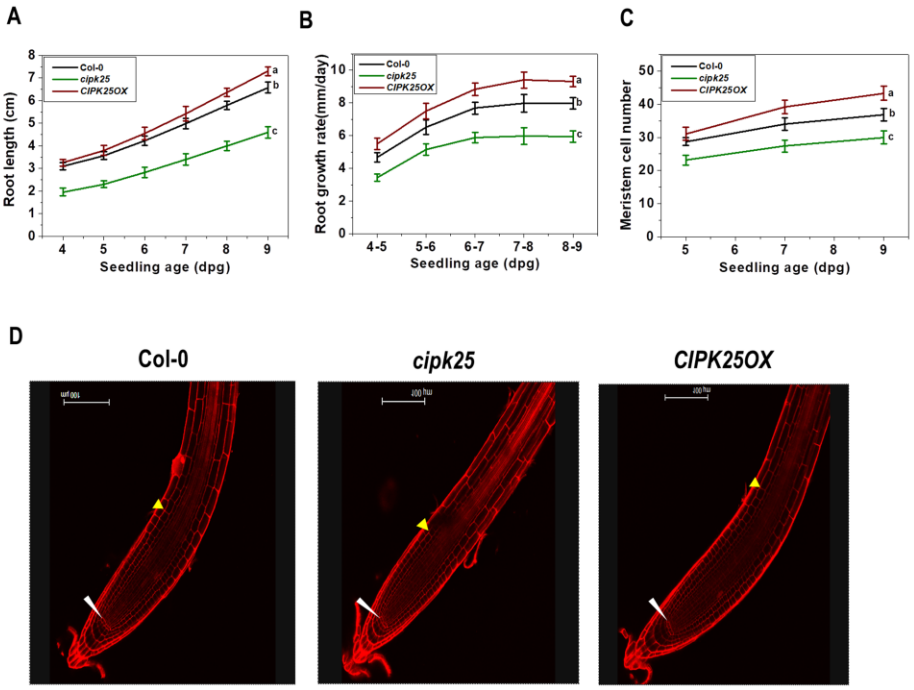

Fig. 2. *cipk25* mutant exhibits slower root growth rate and less root meristem cell number. (A) and (B) Primary root length and growth rate (mm/day) measurements of Col-0, *cipk25* and *CIPK25OX* seedlings vertically grown on ½MS medium. Values are SD± of seventy five samples for each genotype. Different letters indicate significant differences (ANOVA; $P \leq 0.05$) at 9 dpg and 8-9 dpg old seedlings for root length and growth rate. (C) Meristem cell number count in Col-0, *cipk25* and *CIPK25OX* in 5, 7 and 9 dpg old seedlings. Error bars are SD± of n=20. Different letters indicate statistically significant differences among 9 dpg old seedlings (ANOVA; $P \leq 0.05$). (D) Propidium iodide-stained primary roots of 5 dpg old Col-0, *cipk25* and *CIPK25OX* seedlings. White and yellow arrows indicate quiescent center (QC) and the first elongated cortex cell, respectively.

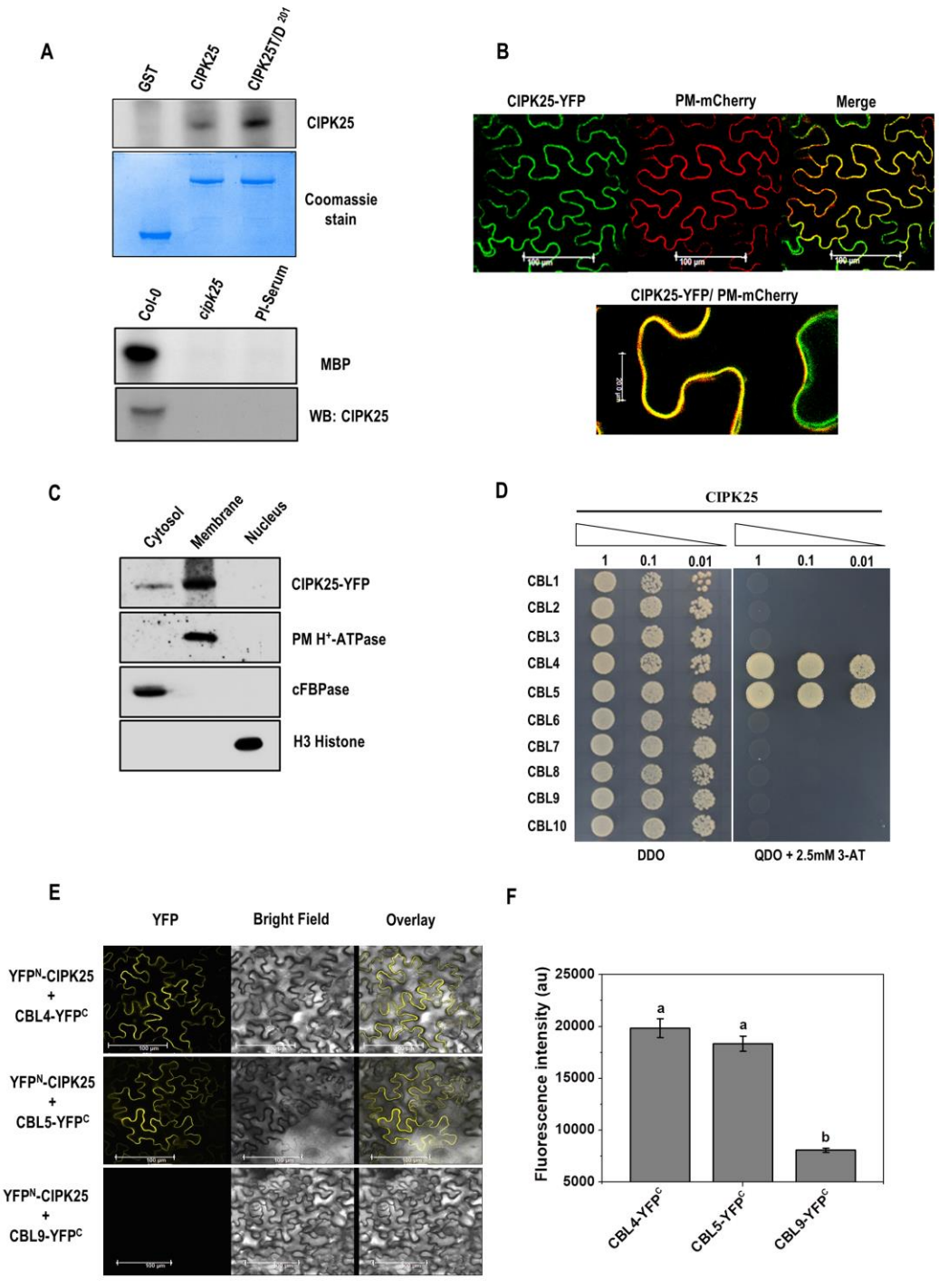

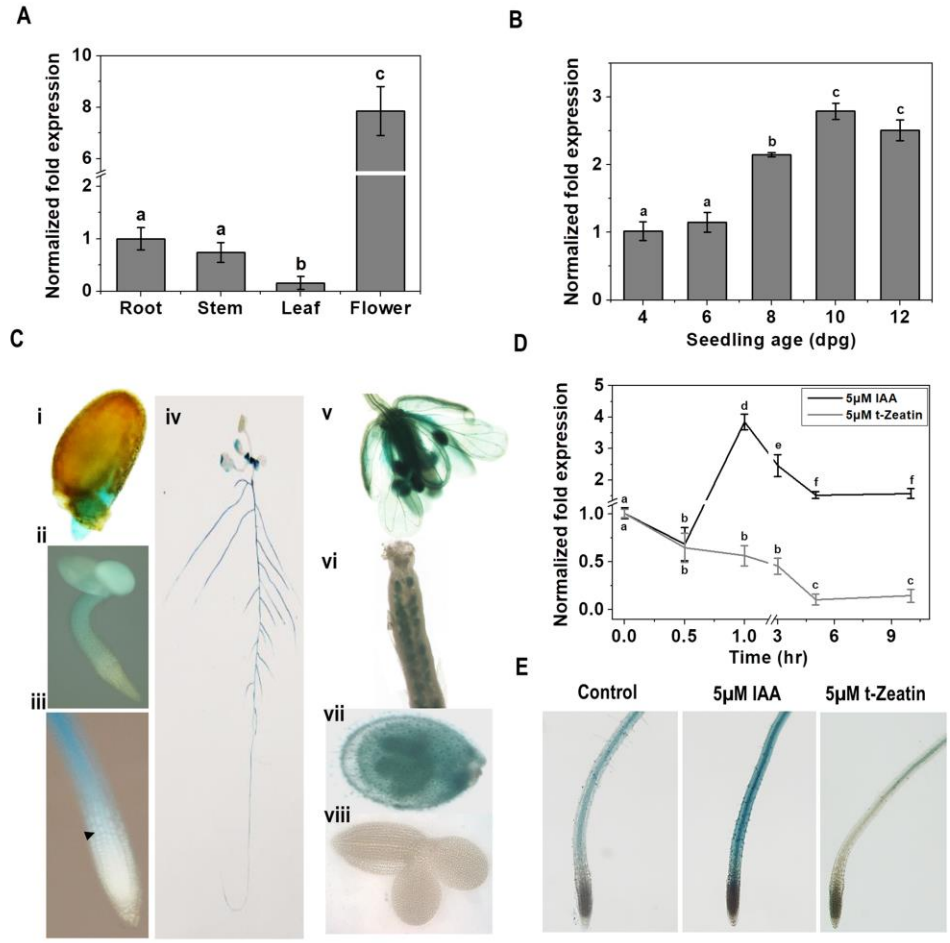

Fig. 4. *CIPK25* gene expression profiles at in different tissues, root growth stages and in response to hormone treatments. CIPK25 gene expression in different tissues (A) and in different root growth stages (B) analyzed by qRT-PCR. *ACTIN2* expression was used for normalization. Error bars SD±, n=3. Different letters indicate significant differences among samples (ANOVA; $P \leq 0.05$). (C) CIPK25 promoter activities were investigated with promoter::reporter gene (GUS) constructs expressed in transgenic plants. Histochemical GUS stainings are shown for (i) radicle of germinating seedling; (ii) 2 dpg old seedling; (iii) primary root tip of 5 dpg old seedling (Arrow indicates first elongated cortex cell); (iv) 10 dpg old seedling; (v) flower; (vi) gynoecium; (vii) immature seeds with embryo; (viii) embryo. (D) Fold change in *CIPK25* expression as analysed by qRT-PCR in roots of 10 dpg old Col-0 seedlings treated with 5μM IAA and 5μM t-Zeatin for different time interval. *ACTIN2* expression was used for normalization. Error bars SD±, n=3. Different letters indicate significant differences among samples (ANOVA; $P \leq 0.05$). (E) *pCIPK25::GUS* expression was visualized in primary roots of 10 dpg old seedlings treated with 5μM IAA for 1 hr and 5μM t-Zeatin for 5hr.

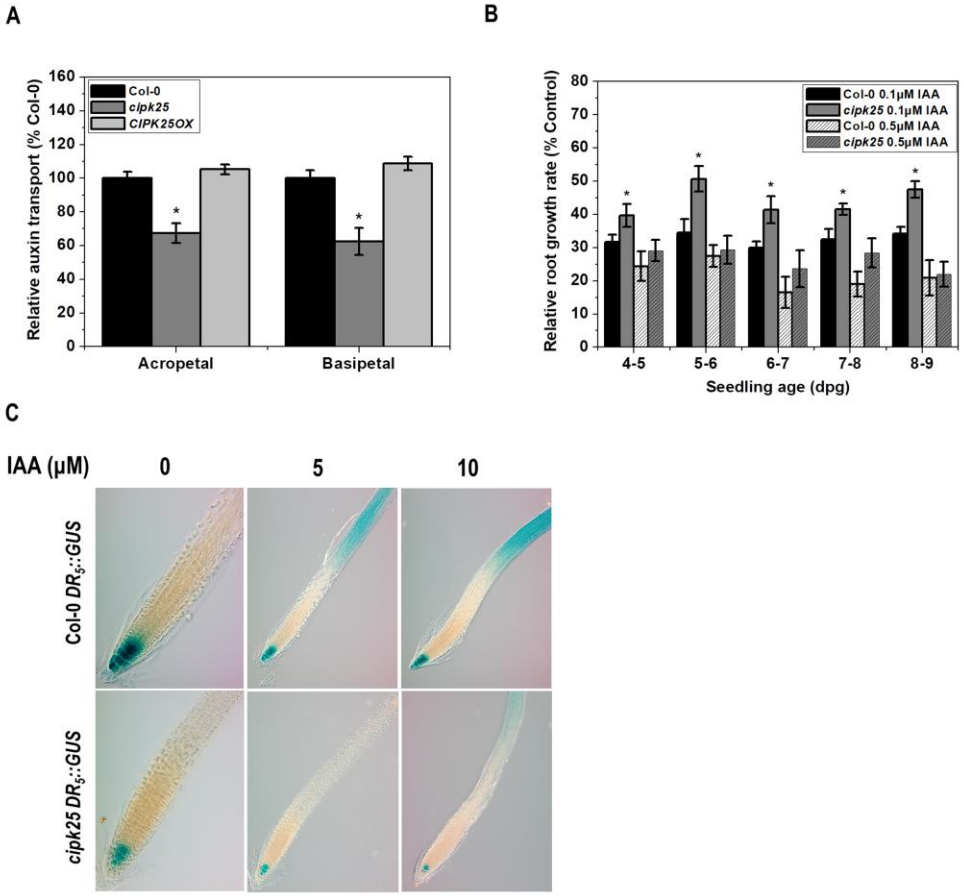

Fig. 5. Auxin transport and auxin-responsive promoter assays in *cipk25*. (A) Comparison of acropetal (rootward) and basipetal (shootward) root auxin transport in 5 dpg old Col-0, *cipk25* and *CIPK25OX* seedlings in a root segment 2 mm below (in acopetal) or above (in basipetal) the site of ^{3}H-IAA application. Data are presented as the percentage auxin transport relative to Col-0. Error bars are SD±, t-test (*P ≤ 0.05) of three measurements of 15 seedlings each. (B) Auxin-mediated root growth rate retardation of Col-0 and *cipk25* in response to 0.1 μM and 0.5 μM auxin treatments. 4 dpg old Col-0, *cipk25* mutant seedlings grown on ½ MS medium were transferred to IAA-free or IAA-containing medium, and grown for an additional 5 days. Relative root growth rate in presence of external IAA was presented as the percent of growth rate (per day) of the same line in control condition (without IAA). The error bars represents SD±, t-test (*P ≤ 0.05), with three replicates of 10 seedlings each. (C) Auxin responsive promoter activity using *DR$_5$::GUS* in Col-0 and *cipk25* mutant. 5 dpg old seedlings were treated with 5μM and 10μM IAA for 2 hrs and stained for GUS activity.

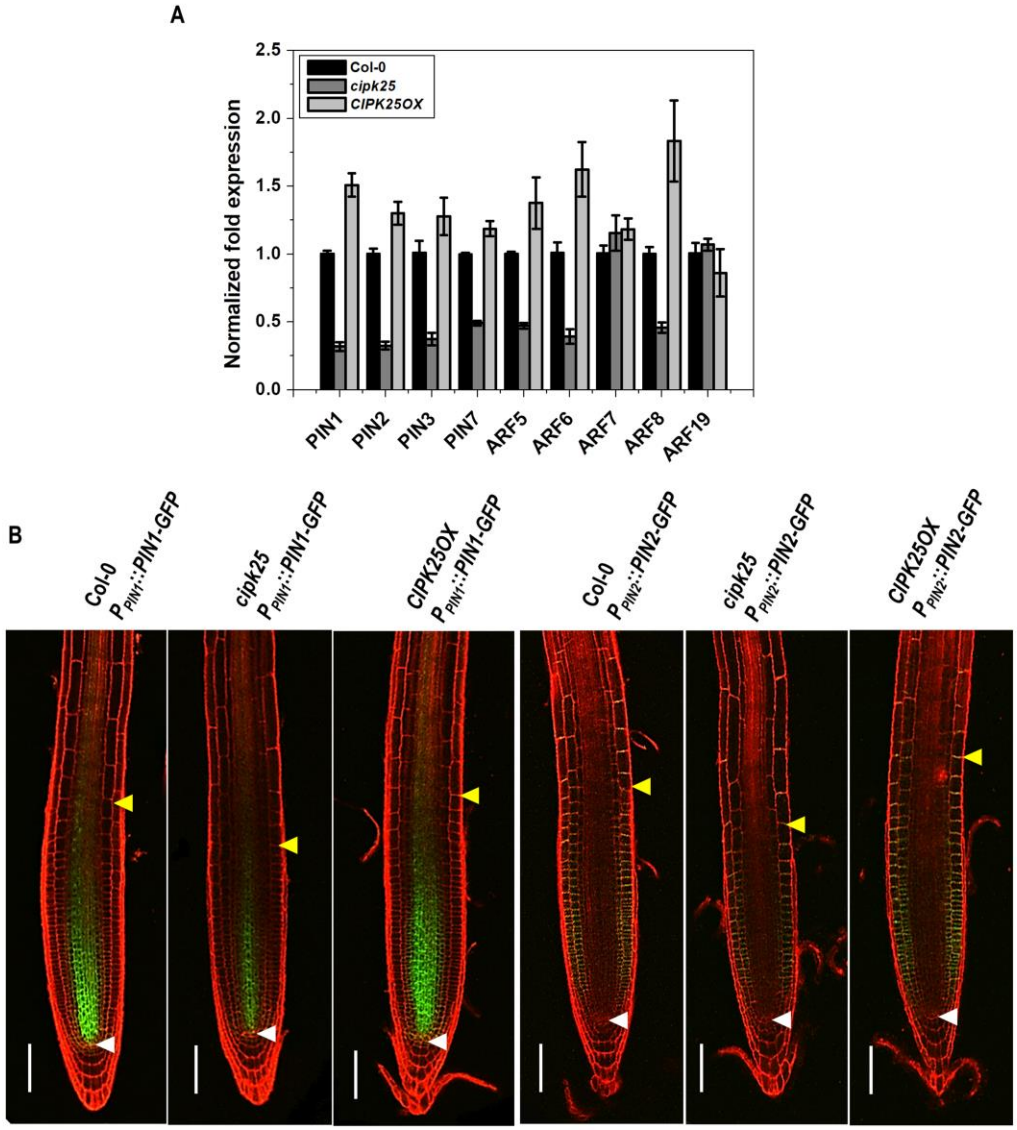

Fig. 6. Expression of auxin response factors (ARFs) and efflux carriers (PINs) in *cipk25*. (A) Relative transcript levels of auxin response factors (*ARF5*, *ARF6*, *ARF7*, *ARF8* and *ARF19*) and efflux carriers (PIN1, PIN2, PIN3 and PIN7) were analyzed by qRT-PCR in roots of 5 dpg old Col-0, *cipk25* and *CIPK25OX* seedlings. *ACTIN2* expression was used for normalization. Error bars represents SD± of three biological replicates with fifteen seedlings for each genotype. (B) Visualization of expressions of auxin efflux carriers PIN1 and PIN2. Fluorescence images from the GFP fusion proteins expressed through the native promoters of individual genes in Col-0, *cipk25* and *CIPK25OX* background. 5 dpg old seedlings were stained with propidium iodide to explore meristem cell profiles and analysed by confocal microscope. Scale bar in confocal images = 100µm. White and yellow arrows indicate quiescent center (QC) and the first elongated cortex cell, respectively.

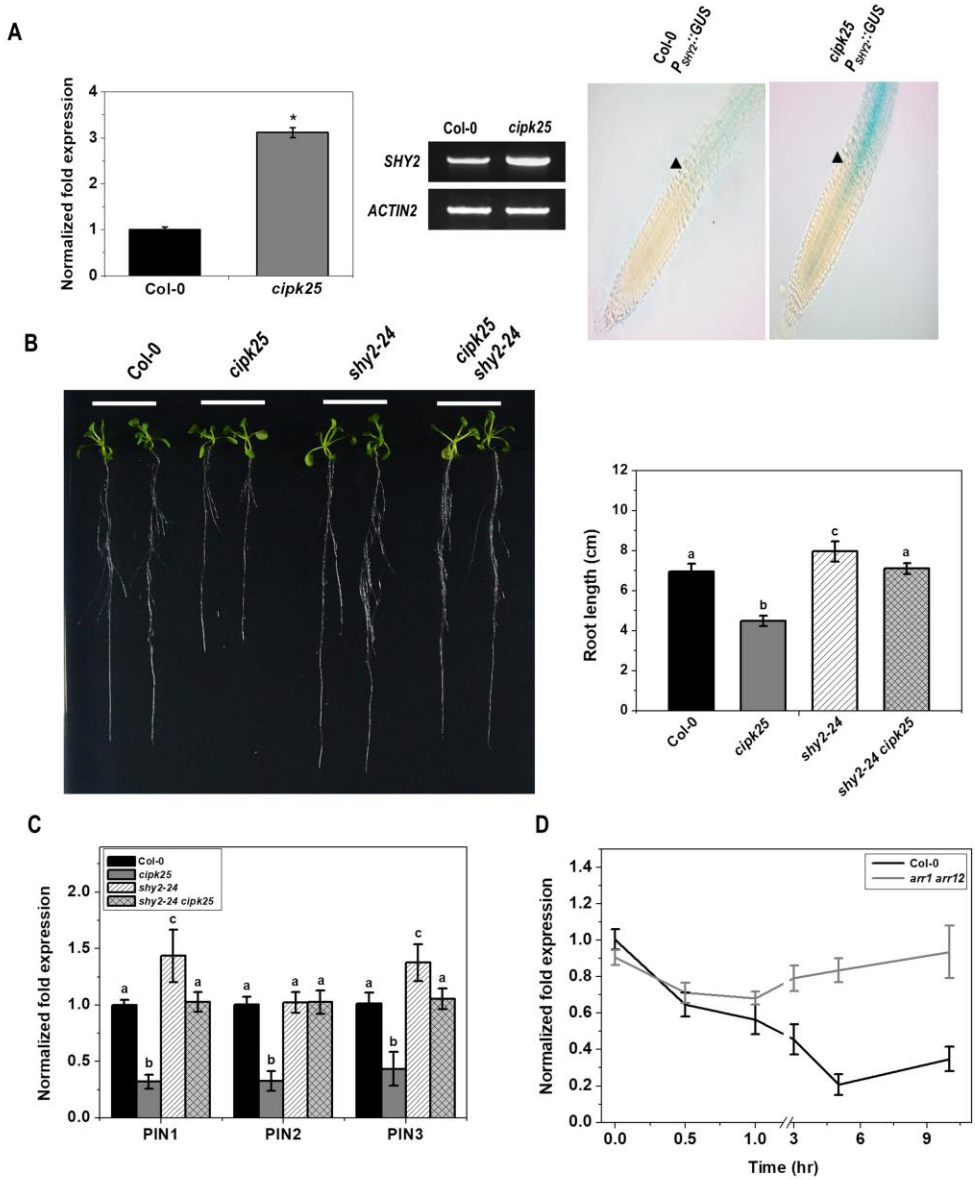

Fig. 7. Genetic interaction of *CIPK25* and *SHY2*. (A) Relative transcript abundance of *SHY2* in 5 dpg old Col-0 and *cipk25* mutant roots was analysed by qRT-PCR and semi-quantitative RT-PCR. *ACTIN2* was used as internal control. Right panel shows histochemical GUS staining of primary roots of 5 dpg-old seedlings expressing GUS reporter under *SHY2* promoter. Arrow shows the first elongated cortex cell. (B) Primary root length phenotype of 10 dpg-old Col-0, *cipk25*, *shy2-24* and *cipk25 shy2-24* mutants vertically grown on ½ MS medium. Right panel shows root length measurement. Error bars represent SD±, n=24. (C) Relative transcript levels of auxin efflux carriers were analysed by qRT-PCR in roots of 5 dpg old Col-0, *cipk25*, *shy2-24* and *cipk25 shy2-24* seedlings. Different letters indicate statistically significant differences by ANOVA, $P \leq 0.05$. Error bars are SD±, n=3. (D) qRT-PCR analysis of the expression levels of *CIPK25* in roots of 10 dpg-old Col-0 and *arr1 arr12* seedlings treated with 5µM t-Zeatin for different time interval. *ACTIN2* expression was used as internal control. Error bars are SD±, n=3.

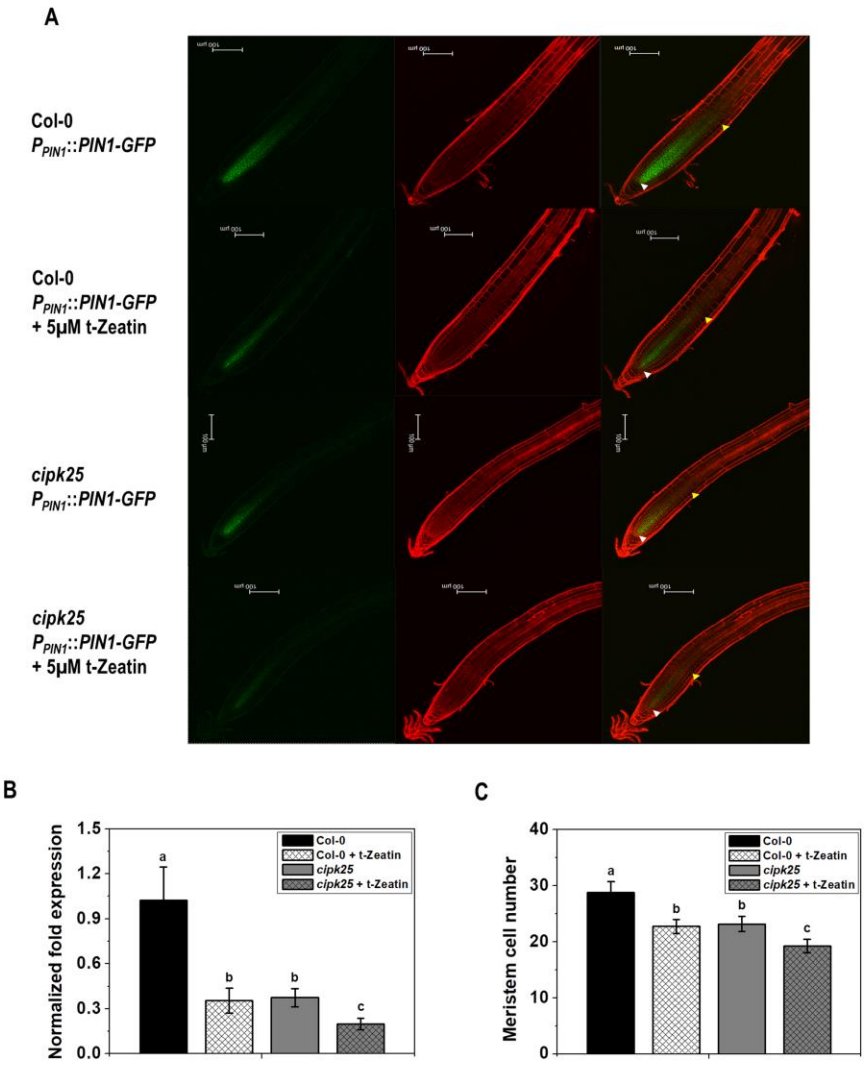

Fig. 8. Cytokinin-responsive PIN1 expression in *cipk25*. (A) Fluorescence images of auxin efflux carrier PIN1-GFP fusion protein driven through its native promoter in Col-0 and *cipk25* seedlings in control condition and in response to cytokinin treatment (5 µM t-Zeatin, 6 hours). Roots of 5 dpg-old seedlings were stained with propidium iodide (PI) for visualizing root cells. White and yellow arrows indicate quiescent center (QC) and the first elongated cortex cell, respectively. Scale bar =100µM. (B) Relative transcript levels of *PIN1* was analysed by qRT-PCR in roots of 5 dpg-old Col-0 and *cipk25* seedlings in control and treated with cytokinin (5 µM t-Zeatin, 6 hours). Error bars are SD± of 3 biological replicates, ANOVA, $P \leq 0.05$. (C) Meristem cell number count in 5 dpg-old Col-0 and *cipk25* seedlings in control condition and in response to cytokinin treatment (5 µM t-Zeatin, 12 hours). Values are mean ± SD of twenty samples each. Different letters indicate significant differences among samples (ANOVA; $P \leq 0.05$).